RSC Advances

PAPER

View Article Online
View Journal | View Issue

Cite this: *RSC Adv.*, 2024, **14**, 32101

Highly sensitive colorimetric detection of Cd(II) based on silica sol modified with dithizone and cationic surfactant†

Arpaporn Litluechai,[a] Arreerat Prompa,[a] Pikaned Uppachai,[b] Wirat Jarernboon,[c] Nutthaya Butwong[d] and Siriboon Mukdasai *[a]

The cadmium ion (Cd^{2+}) is highly poisonous and nondegradable and easily bioaccumulates through the food chain. Therefore, it is crucial to develop cost-effective chemical sensors for Cd^{2+} with fast response time, high selectivity, and very low detection limits. In this study, a colorimetric sensor for the determination of Cd^{2+} was fabricated by modifying silica sol with dodecyltrimethylammonium bromide (DTAB) and dithizone (DZ). Cd^{2+} formed a complex with DZ, changing the solution color immediately from purple to orange prior to detection using ultraviolet-visible spectrophotometry and a customized Cd analyzer for the precipitate. Under the optimum conditions, the developed Cd^{2+} sensor had a linear range of 0.01–0.25 mg L^{-1}, a low limit of detection of 5.0 μg L^{-1}, and outstanding repeatability. This sensor also showed good precision, with the relative standard deviations of less than 2.59% and 3.24% for the intra- and inter-day data, respectively. The proposed colorimetric method was successfully applied to determine Cd^{2+} in environmental water samples, and the results were comparable to those obtained using standard atomic absorption spectrometry. Moreover, quantitative analysis was conducted using the customized Cd analyzer to estimate the color intensity change, without requiring sophisticated scientific instruments. This colorimetric sensor can be used for the portable, cost-effective, and rapid on-site detection of Cd^{2+} in environmental water samples.

Received 30th May 2024
Accepted 3rd October 2024

DOI: 10.1039/d4ra03983a

rsc.li/rsc-advances

1. Introduction

The cadmium ion (Cd^{2+}) is very toxic because it exhibits carcinogenicity and teratogenicity, severely impacting the kidneys, liver, and reproductive organs in humans.[1,2] Moreover, it easily accumulates in the human body through the food chain owing to its nondegradable nature.[3,4] Common sources of Cd^{2+} in the environment are paint factory effluents, plastics, hardware fittings, nuclear reactor control rods, radium detection devices, photoconductive elements in televisions, and electronic waste (*e.g.*, mobile phones and their batteries as well as computer circuit boards).[5] The World Health Organization established the maximum residue limit of Cd^{2+} in drinking water to be 0.003–0.005 mg L^{-1}.[6] Therefore, it is crucial to develop highly selective, rapid, and cost-effective chemical sensors with very low detection limits for Cd^{2+} in environmental water.

Reported high-performance techniques for Cd determination are based on inductively coupled plasma-mass spectrometry,[7–9] inductively coupled plasma-atomic emission spectrometry,[10] inductively coupled plasma-optical emission spectrometry,[11] atomic absorption spectroscopy,[12–15] and electrochemistry.[16–18] However, these techniques require highly trained operators, the analysis process is time-consuming, and the instrument is typically expensive and nonportable. In recent years, colorimetric methods have received great attention due to being simple, inexpensive, and effective for quantitative analyses. They also allow detection by the naked eye without specialized detectors. Colorimetric methods for detecting heavy metals rely on the different chromogenic materials. The main content of this work focused on the aggregation (or the reverse dissociation process) of noble metals and nanoparticles such as gold nanoparticles, silver nanoparticles, and silica sol.[19–24]

Silica sol (also called colloidal silica) has desirable properties for colorimetric sensors. As a nanocolloid having a siloxane network structure (Si–O–Si),[25] it is easily synthesized using the Stöber method that involves the hydrolysis and condensation of tetraethoxysilane (TEOS) and L-arginine (L-arg).[25–27] This method is popular because the sol–gel process is inexpensive, easy, and highly efficient compared with other methods. Particles in the

[a]*Materials Chemistry Research Center, Department of Chemistry and Center of Excellence for Innovation in Chemistry, Faculty of Science, Khon Kaen University, Khon Kaen 40002, Thailand*

[b]*Department of Applied Physics, Faculty of Engineering, Rajamangala University of Technology Isan, Khon Kaen Campus, Khon Kaen 40000, Thailand*

[c]*Department of Physics, Faculty of Science, Khon Kaen University, Muang, Khon Kaen, 40002, Thailand*

[d]*Applied Chemistry Department, Faculty of Science and Liberal Arts, Rajamangala University of Technology Isan, Nakhon Ratchasima 30000, Thailand*

† Electronic supplementary information (ESI) available. See DOI: https://doi.org/10.1039/d4ra03983a

obtained silica sol are small and well dispersed, resulting in a large specific surface area. Notably, silica sol can be directly used as a sorbent without the energy-intensive and/or lengthy drying or calcination steps. We have previously used silica sol as a new sorbent for detecting trace levels of Fe^{2+} (ref. 27) and Cd^{2+} which use the trimethyl tetradecyl ammonium bromide (TTAB) and murexide on silica sol as a colorimetric probe.[24]

Cationic surfactants can facilitate the aggregation of silica sol and enhance its surface properties through electrostatic interactions between the positively charged surfactant and negatively charged silica sol particles.[24,27–29] In addition, the sensitivity and selectivity of nanoparticle-based colorimetric sensors can be improved by modifying the particle surface using specific ligands. The adsorption of metal cations on silica sol occurs *via* electrostatic interactions between the hydroxyl groups of silanol and metal cations. However, the ligands should be carefully chosen to enhance metal adsorption.

In colorimetric detection, the derivatization of Cd^{2+} with an appropriate ligand produces complexes that display different colors. It also enhances sensitivity and selectivity for Cd^{2+} detection. The following ligands have been reported to form complexes with Cd^{2+}: 5,7-dibromo-8-hydroxyquinoline,[30] ammonium pyrrolidinedithiocarbamate,[31], (*E*)-*N*′-(2-hydroxy-5-nitrobenzylidene)isonicotinoylhydrazone, 2-(4-fluoro (benzlideneamino)benzenothiol),[32] 1-(2-pyridylazo)-2-naphthol,[33] and murexide.[24] To the best of our knowledge, there have been some reports on using dithizone (DZ) as a ligand for Cd^{2+} detection, because the sulfur and nitrogen atoms in DZ can react with metal ions by donating free electron pairs.[34,35] Notably, DZ binds strongly with Cd^{2+} with a high complex formation constant (log K_f) under suitable conditions.[36,37]

In this study, we developed an effective, simple, and portable colorimetric sensor for the detection of Cd^{2+}. A probe was prepared by modifying silica sol with DZ and dodecyltrimethylammonium bromide (DTAB, a cationic surfactant). This DTAB/DZ/silica sol probe is sensitive and selective to Cd^{2+}. Specifically, the presence of Cd^{2+} caused a color change of the aqueous probe solution from purple to orange, and this color change was measured by spectrophotometry at 435 nm for quantification and a customized Cd analyzer. The proposed colorimetric probe was successfully applied to the determination of Cd^{2+} in environmental water samples.

2. Experimental section

2.1 Materials and chemicals

All chemicals were of analytical reagent grade except for TEOS (gas chromatography grade, Sigma-Aldrich). Cadmium chloride ($CdCl_2$) was obtained from HIMEDIA. Cetyltrimethylammonium bromide (CTAB) and Dithizone (DZ) were purchased from Fluka. Cobalt(II) chloride hexahydrate ($CoCl_2 \cdot 6H_2O$), copper(II) sulfate pentahydrate ($CuSO_4 \cdot 5H_2O$), ammonium ferrous sulfate hexahydrate ($Fe(NH_4)_2(SO_4)_2 \cdot 6H_2O$), and potassium chloride (KCl) were obtained from CARLO ERBA. L-Arginine ($C_6H_{14}N_4O_2$) was obtained from ACROS. Sodium dihydrogen phosphate dihydrate ($NaH_2PO_4 \cdot 2H_2O$) and trimethyl tetradecyl ammonium bromide (TTAB) were obtained from KEMAUS.

Sodium acetate and acetic acid were purchased from Merck. Dodecyltrimethylammonium bromide (DTAB), nitric acid (HNO_3, 65%), and methanol (MeOH) were obtained from Sigma-Aldrich. Magnesium sulfate ($MgSO_4$), *ortho*-phosphoric acid (H_3PO_4), and sulfuric acid (H_2SO_4) were acquired from QRëC. Deionized water produced from ELGA (PURELAB Ultra Analytic) with a specific resistivity of 18.2 MΩ cm was used in all experiments.

A Cd^{2+} stock solution (1.0 mmol L^{-1}) was prepared by dissolving an appropriate amount of Cd^{2+} in 0.1 mol L^{-1} H_2SO_4. Every day, Cd^{2+} working solutions were prepared by the stepwise dilution of this stock solution with deionized water. Phosphate buffers at various pH values (pH 2.0–3.0) were prepared by mixing 0.1 mol L^{-1} H_3PO_4 and 0.1 mol L^{-1} NaH_2PO_4 in different ratios. The acetate buffer solution at various pH values (pH 4.0–6.0) were prepared by 0.1 mol L^{-1} acetic acid and sodium acetate in different ratios. All glassware was stored in 10% (v/v) HNO_3 for at least 24 h and washed thoroughly with deionized water before use.

2.2 Instrumentation

Absorption spectra were recorded on an ultraviolet-visible (UV-vis) spectrophotometer (Cary 60 Agilent, Australia) by scanning the reaction solution in a 3.5 mL quartz cuvette from 380 to 490 nm. Fourier-transform infrared spectroscopy was performed using a Bruker Tensor 27 spectrometer. The zeta potential was measured using a Zetasizer Nano ZS (Malvern, UK) to confirm the charge on the silica sol surface. The morphology of silica sol was studied using focused ion beam-scanning electron microscopy (FIB-SEM; Helios NanoLab G3 CX, FEI, USA). A customized Cd analyzer based on RGB analysis was used to measure the change in red (R) color intensity.

2.3 Synthesis of silica sol

Silica sol was prepared using the Stöber method according to our previous reports, based on the hydrolysis and condensation of TEOS and L-arg.[24,27] L-arg (0.09 g) was dissolved in deionized water (250 mL) and stirred at 60 °C for 30 min in an oil bath. Then, TEOS (18.66 g) was added. The mixture was stirred continuously at 60 °C and 300 rpm for 26 h using a magnetic stirrer, and then kept at room temperature for subsequent experiments.

2.4 Colorimetric sensor for Cd^{2+} detection

The mechanism of the colorimetric DTAB/DZ/silica sol probe is illustrated in Fig. 1. To prepare this probe, silica sol (2000 μL), DZ (0.09 mg L^{-1}), and DTAB (1000 μL) were added to a 15 mL centrifuge tube. Next, a standard solution containing 0.09 mg L^{-1} Cd^{2+} was added to the centrifuge tube, and it was then diluted with a 0.1 mol L^{-1} phosphate buffer solution (pH 3.0, up to 10 mL) through manual shaking. The obtained colloidal solution (DTAB/[Cd^{2+}-DZ]/silica sol) was self-assembled and precipitated to the bottom of the centrifuge tube under gravity. Finally, the absorbance of the upper phase was measured at

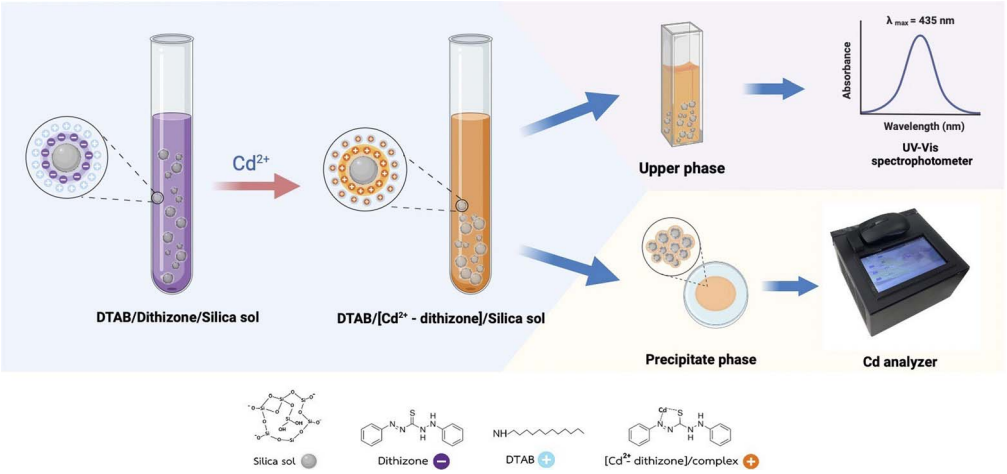

Fig. 1 Proposed colorimetric sensor for Cd^{2+} determination based on dodecyltrimethylammonium bromide (DTAB)/dithizone (DZ)/silica sol.

435 nm. The efficiency in the adsorption or extraction of the formed [Cd^{2+}-DZ] complex was evaluated using %adsorption defined in eqn (1):[38–40]

$$\%\text{Adsorption} = [(A_0 - A_t)/A_0] \times 100 \quad (1)$$

where A_0 and A_t are absorbances of the [Cd^{2+}-DZ] complex before and after adsorption on the colorimetric probe, respectively. The precipitate was filtered through a membrane filter and evaluated using a customized Cd analyzer.

In this work, Cd quantification was performed by the expression of calibration curves using a customized Cd analyzer to evaluate the channels red (R), green (G) and blue (B). The R channel displays a well-linear response with an acceptable correlation coefficient (R^2) when compared with others. Because the color of cadmium complex was related to the R color. Thus, the R value was used as an analytical signal for the experiments.

2.5 Sample analysis

The prepared colorimetric sensor was used to detect Cd^{2+} in four environmental water samples (W1–W4) including tap water (W1), natural water (W2), and wastewater (W3–4). All samples were collected from Khon Kaen Province, Thailand and first passed through a 0.45 μm membrane filter (VertiClean™ NYLON) prior to Cd^{2+} detection.

3. Results and discussion

3.1 Characterization of DTAB/DZ/silica sol probe

The morphologies of silica sol, DTAB/silica sol, and DTAB/[Cd^{2+}-DZ]/silica sol were observed through FIB-SEM. According to the surface morphology in Fig. 2A, the silica sol particles were spherical and had a diameter of 100 ± 2.35 nm (n = 20). After adding DTAB, DTAB/silica sol (particle size: 50 ± 4.25 μm, n = 20) formed large rod-shaped particles owing to the aggregation of DTAB and silica sol (Fig. 2B). The presence of the [Cd^{2+}-DZ] complex promoted the aggregation of DTAB/[Cd^{2+}-DZ]/silica sol, as shown in Fig. 2C.

To confirm the adsorption of [Cd^{2+}-DZ] onto DTAB/silica sol, the surface charge of the probe particles was studied using a zeta potential analyzer. Pure silica sol had a negative potential (−31.23 mV), after the addition of DTAB which has a positive charge, the potential was slightly raised to positive value (−0.11 mV). When silica sol was combined with [Cd^{2+}-DZ], a positive potential (2.13 mV) was observed instead. Furthermore, DTAB/[Cd^{2+}-DZ]/silica sol had a more positive potential (5.07 mV). These changes suggest that the [Cd^{2+}-DZ] complex was adsorbed on DTAB/silica sol.

3.2 Optimization of colorimetric probe for Cd^{2+} detection

3.2.1 Effects of pH and time. The pH of the aqueous solution plays a key role in the speciation of chelating agents,

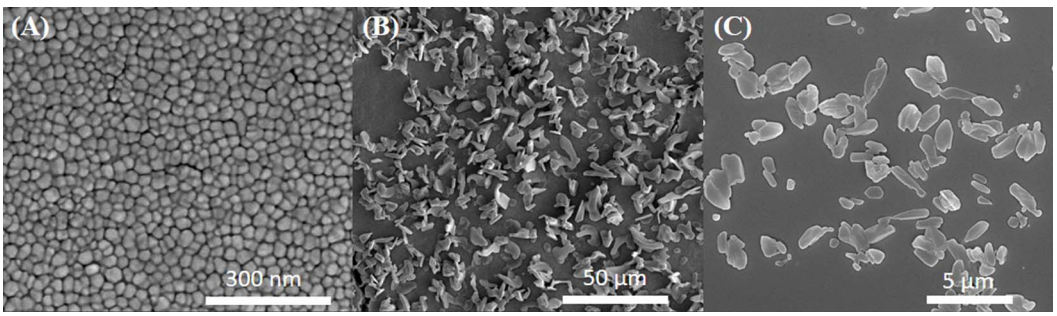

Fig. 2 SEM images of (A) silica sol, (B) DTAB/silica sol, and (C) DTAB/[Cd^{2+}-DZ]/silica sol.

complex formation, and extraction efficiency. Here, complex formation between DZ and Cd^{2+} was investigated in the pH range of 2.0–6.0 using different buffer solutions (0.1 mol L^{-1} phosphate buffer and acetate buffer). As shown in Fig. S1A,† the [Cd^{2+}-DZ] complex solution achieved maximum absorbance at pH 3.0 and a slightly lower absorbance at higher pH. Therefore, the phosphate buffer at pH 3.0 was selected for further experiments.

To study stability of the [Cd^{2+}-DZ] complex, its absorbance was monitored for 50 min. The absorbance increased during the first 30 min and then decreased slightly (Fig. S1B†). Thus, in the subsequent experiments, the detection of Cd^{2+} was carried out at 30 min after mixing.

3.2.2 Effect of probe volume. The effect of the amount of sorbent on extraction efficiency was studied by varying the volume of silica sol from 1.0 to 6.0 mL and measuring % adsorption and red (R) intensity. The %adsorption (obtained *via* UV-vis spectrophotometry) increased significantly with the increase in the silica sol volume from 1.0 to 3.0 mL and decreased when the volume was above 3 mL, as shown in Fig. 3A. The *R* intensity (measured for the precipitate on the membrane filter) was evaluated using a customized Cd analyzer based on the color change. The results showed a trend similar to that of %adsorption. Thus, the of silica sol volume was fixed at 3.0 mL in the subsequent experiments.

3.2.3 Effect of surfactant. Surfactants are stabilizing agents that induce the aggregation of [Cd^{2+}-DZ] complexes and nanoparticles (such as silica sol).[24,27] Three cationic surfactants, namely, CTAB, DTAB, and TTAB, were tested. The addition of a cationic surfactant made the solution cloudy, because the surfactant aggregated with [Cd^{2+}-DZ] and silica sol to produce surfactant/[Cd^{2+}-DZ]/silica sol. Fig. 3B shows the %adsorption of [Cd^{2+}-DZ] on silica sol modified with different cationic surfactants. It was obvious that DTAB caused the highest % adsorption. The color intensity of the precipitate on the membrane filter was evaluated using a customized Cd analyzer, and the results showed a trend similar to that of %adsorption. Therefore, DTAB was selected as the surfactant in the subsequent experiments.

Next, the concentration of DTAB was studied in the 0.010–0.120 mol L^{-1} range, which is at or above the critical micellar concentration of DTAB (0.01401 mol L^{-1}).[41] The results (Fig. 3C) show that the %adsorption of the [Cd^{2+}-DZ] complex increased significantly upon increasing the DTAB concentration from 0.01

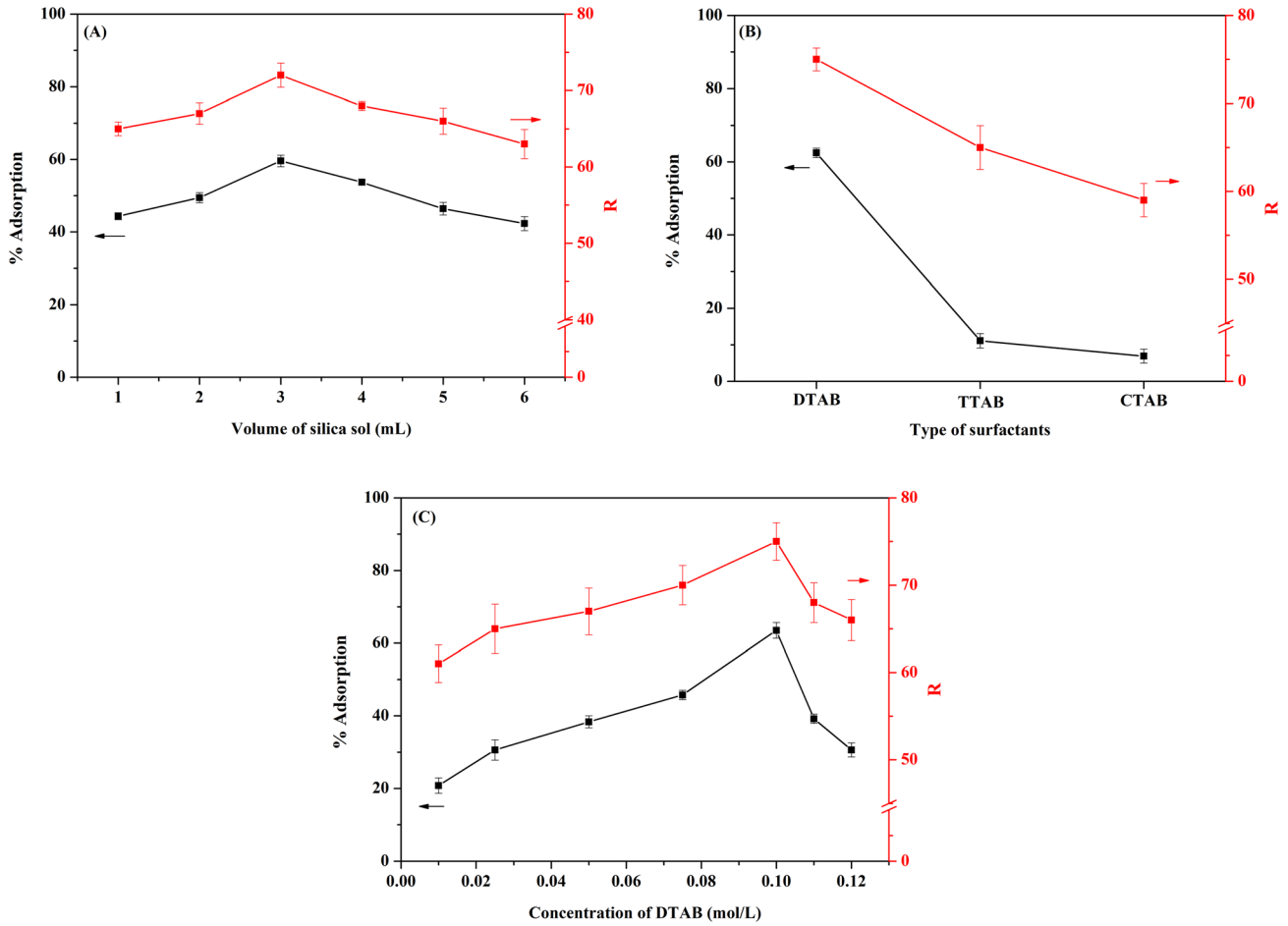

Fig. 3 Effects of (A) volume of silica sol, (B) type of surfactant, and (C) concentration of DTAB on the colorimetric sensor (DTAB/DZ/silica sol) for Cd^{2+} determination.

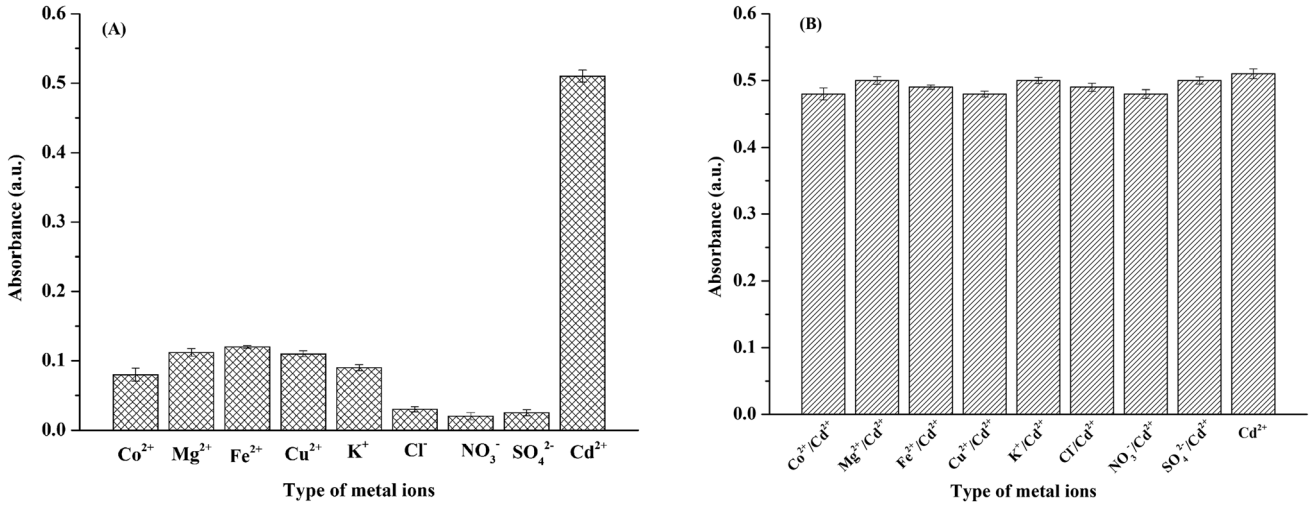

Fig. 4 Absorbance of the colorimetric probe in the presence of (A) one ionic species at 0.09 mg L^{-1} and (B) Cd^{2+} (0.09 mg L^{-1}) and a coexisting ion (0.09 mg L^{-1}).

to 0.1 mol L^{-1}, similar to the trend of *R* intensity measured for the precipitate. The highest %adsorption and *R* intensity were obtained at 0.1 mol L^{-1} DTAB. Above this concentration, both values decreased significantly because of the dilution effect. Thus, 0.1 mol L^{-1} DTAB was selected for further study.

3.3 Selectivity toward Cd^{2+}

Selectivity is a key parameter of colorimetric sensors because real environmental samples tend to contain interfering species such as other cations and anions. Therefore, we tested the probe's selectivity toward other common ions found in water samples (Co^{2+}, Mg^{2+}, Fe^{2+}, Cu^{2+}, K^{+}, Cl^{-}, NO_3^{-}, and SO_4^{2-}). Two sets of experiments were carried out. (i) The DTAB/DZ/silica sol probe was mixed with a single ionic species (Cd^{2+} or coexisting ions) at 0.09 mg L^{-1}. The corresponding absorbance intensities are shown in Fig. 4A. Only Cd^{2+} produced an orange complex with strong absorption, indicating that this ion alone substantially interacted with the DTAB/DZ/silica sol probe. (ii) A solution containing Cd^{2+} and a coexisting ion (both at 0.09 mg L^{-1}) was tested. As shown in Fig. 4B, all other ions had a negligible effect on absorbance. In summary, the proposed colorimetric sensor exhibited excellent Cd^{2+} selectivity.

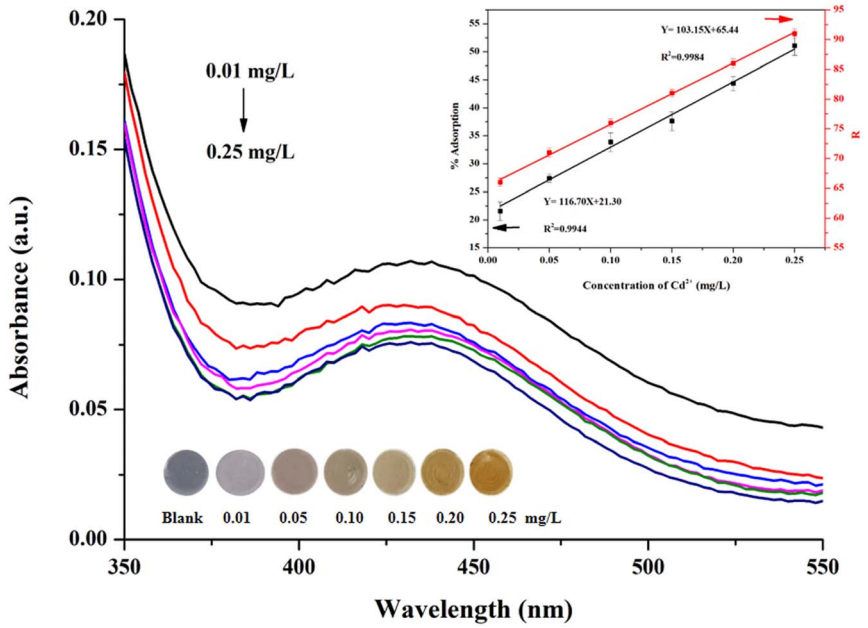

Fig. 5 Quantitative Cd^{2+} detection using the colorimetric sensor. (A) Absorption spectra of DTAB/[Cd^{2+}-DZ]/silica sol at various Cd^{2+} concentrations (inset: photographic images). Peak wavelength: 435 nm. (B) Calibration plots for %adsorption (left *y*-axis) and *R* intensity (right *y*-axis) versus Cd^{2+} concentration.

Table 1 Different colorimetric sensors for Cd^{2+} detection

Method	Colorimetric probe	LOD	Sample	Reference
Colorimetric	Chitosan-dithiocarbamate-modified gold nanoparticles	7.06 μg L^{-1} (0.063 μM)	Tap water	42
Colorimetric	1-Amino-2-naphthol-4-sulfonic-acid-functionalized silver nanoparticles	0.087 μM	Milk powder, serum, and lake water	43
Colorimetric	Silver nanoparticles capped with chalcone carboxylic acid	0.13 μM	Drinking water and lake water	44
Colorimetric	TTAB/murexide/silica sol	0.21 μM	Rice	24
Colorimetric	DTAB/DZ/silica sol	5 μg L^{-1} (44.5 nM)	Environmental water	This work

3.4 Analytical performance

The analytical performance of the proposed DTAB/DZ/silica sol colorimetric probe was investigated for Cd^{2+} solutions at various concentrations under the optimized experimental conditions through UV-vis spectroscopy and by using the customized Cd analyzer. The obtained absorption spectra are shown in Fig. 5A. The absorbance at 435 nm decreased as the Cd^{2+} concentration increased from 0.01 to 0.25 mg L^{-1}. The linear range of %adsorption was 0.01–0.25 mg L^{-1} Cd^{2+} with a regression equation of $Y = 116.70\ X + 21.30$, and the determination coefficient (R^2) was 0.9944 (Fig. 5B).

Moreover, the relationship between the R intensity and Cd^{2+} concentration was evaluated by taking a digital photograph and measuring the color intensity using the customized Cd analyzer (Fig. 5B). The regression equation was $Y = 103.15X + 65.44$, with $R^2 = 0.9984$.

The limit of detection (LOD) and limit of quantitation (LOQ) were calculated on the basis of the ratio of the standard deviation of the blank solution (s) to the slope of the calibration plot (m) at 3 and 10, and the obtained values were 5.0 and 18 μg L^{-1}, respectively. The precision of the DTAB/DZ/silica sol probe was expressed as the relative standard deviation in percentage (% RSD, $n = 5$) when measuring 0.09 mg L^{-1} Cd^{2+} in one (intra-day) and five consecutive days (inter-day). The results indicate that the proposed probe has good precision with %RSD values less than 7.67%. A comparison of the proposed sensor with other colorimetry-based sensors for the detection of Cd^{2+} is presented in Table 1. The LODs of the proposed sensor are comparable to those in the literature, thus serving as a potential alternative medium for Cd^{2+} detection.

3.5 Determination of Cd^{2+} in real water samples

The proposed colorimetric sensor (DTAB/DZ/silica sol) was used to detect Cd^{2+} contamination in environmental water samples. However, Cd^{2+} was not detected in any of the four as-collected samples. To evaluate recovery, Cd^{2+} was spiked at three concentrations (0.050, 0.125, and 0.250 mg L^{-1}) into the samples before performing additional determination experiments. The recoveries are summarized in Table 2. High recoveries were obtained in the acceptable range of 96.8–105.6% with an RSD below 4.0%. These results indicated that the proposed colorimetric sensor suffered no matrix effect. A t-test was

Table 2 Performance of the colorimetric and FAAS methods for the determination of Cd^{2+} in spiked environmental water samples including tap water (W1), natural water (W2), and wastewater (W3–4)

	Proposed colorimetric sensor				FAAS method		
Samples	Spiked (mM)	Found[b] (mM)	Recovery[c] (%)	%RSD[d]	Found[b] (mM)	Recovery[c] (%)	%RSD[d]
W1	—	nd [a]	—	—	nd	—	—
	0.050	0.051	101.7	1.6	0.049	98.0	3.8
	0.125	0.128	102.8	1.2	0.123	98.4	2.1
	0.250	0.259	103.5	1.5	0.245	98.0	1.9
W2	—	nd	—	—	nd	—	—
	0.050	0.048	96.8	1.3	0.045	90.0	4.2
	0.125	0.130	104.1	2.6	0.122	97.6	1.6
	0.250	0.251	100.3	2.4	0.252	100.8	2.3
W3	—	nd	—	—	nd	—	—
	0.050	0.048	96.8	3.0	0.047	94.0	3.5
	0.125	0.132	105.6	2.3	0.121	96.8	1.7
	0.250	0.259	103.7	1.8	0.243	97.2	2.4
W4	—	nd	—	—	nd	—	—
	0.050	0.049	98.0	2.1	0.044	88.0	3.1
	0.125	0.124	99.2	3.9	0.123	98.4	2.3
	0.250	0.252	100.8	2.5	0.249	99.6	2.4

[a] nd: not detected. [b] Detected amount. [c] Recovery = $[(C_{detected} - C_{sample})/C_{spiked}] \times 100$. [d] $n = 3$.

conducted to compare the accuracy of the proposed colorimetric and standard flame atomic absorption spectroscopy (FAAS) methods, considering a *p*-value of 0.05 (at the 95% confidence limit). The calculated *t* value (*t*-cal = 1.35) did not exceed the tabulated *t* value (*t*-table = 2.92), indicating that there was no significant difference between the two methods.

4. Conclusion

A selective and sensitive colorimetric sensor was developed for detecting Cd^{2+} *via* complexation with DZ. The colorimetric probe was fabricated by applying self-assembled DTAB and DZ on a silica sol surface. In the presence of Cd^{2+}, the probe immediately changed color from purple to orange owing to the complexation of Cd^{2+} with DZ, and an orange precipitate of DTAB/[Cd^{2+}-DZ]/silica sol was formed simultaneously. Silica sol enhanced detection sensitivity *via* adsorption. The quantitative determination of Cd^{2+} was performed through UV-vis spectrophotometry and a customized Cd analyzer. The proposed method was sensitive, with an LOD of 5.0 μg L^{-1} that equals the permissible level of Cd in drinking water. When the colorimetric sensor was applied to environmental water samples, the results were comparable to those of the standard FAAS method, providing highly satisfactory recoveries. Therefore, this colorimetric sensor has great potential for the portable, cost-effective, and rapid on-site detection of Cd^{2+}.

Data availability

The data supporting this article have been included as part of the ESI.†

Author contributions

Arpaporn Litluechai: conceptualization, methodology, writing – original draft. Arreerat Prompa: methodology, validation. Pikaned Uppachai: methodology, validation. Wirat Jarernboon: methodology, validation. Nutthaya Butwong: methodology, validation. Siriboon Mukdasai: conceptualization, supervision, writing – review & editing.

Conflicts of interest

There are no conflicts to declare.

Acknowledgements

Financial supports from Materials Chemistry Research Center (MCRC) and the Center of Excellence for Innovation in Chemistry (PERCH-CIC), Ministry of Higher Education, Science, Research and Innovative, Thailand are gratefully acknowledged. S. Mukdasai also would like to acknowledge the Fundamental Fund of Khon Kaen University which has received funding support from the National Science Research and Innovation Fund (NSRF).

References

1 J. Y. Cabon, *Spectrochim. Acta Part B At. Spectrosc.*, 2002, **57**(3), 513–524.
2 M. Xu, P. Hadi, G. Chen and G. McKay, *J. Hazard. Mater.*, 2014, **273**, 118–123.
3 G. Lee, Z. Suonan, S. H. Kim, D. W. Hwang and K. S. Lee, *Mar. Pollut. Bull.*, 2019, **149**, 110509.
4 M. P. Waalkes, *J. Inorg. Biochem.*, 2000, **79**(1–4), 241–244.
5 L. Wu, X. Fu, H. Liu, J. Li and Y. Song, *Anal. Chim. Acta*, 2014, **851**, 43–48.
6 World Health Organization, *Guidelines for drinking-water quality: fourth edition incorporating first addendum*, 2017, https://iris.who.int/handle/10665/254637.
7 N. Zhang, K. Shen, X. Yang, Z. Li, T. Zhou, Y. Zhang, Q. Sheng and J. Zheng, *Food Chem.*, 2018, **264**, 462–470.
8 G. M. Lo Dico, F. Galvano, G. Dugo, C. D'ascenzi, A. Macaluso, A. Vella, G. Giangrosso, G. Cammilleri and V. Ferrantelli, *Food Chem.*, 2018, **245**, 1163–1168.
9 R. S. Lamarca, S. D. S. Ferreira, É. R. Paganini, N. D. S. Ferreira, S. C. Ayala-Durán, G. Isquibola, *et al.*, *J. Mol. Liq.*, 2024, **398**, 124264.
10 M. Zougagh, *Talanta*, 2002, **56**(4), 753–761.
11 Z. Cai and Z. Wang, *Anal. Chim. Acta*, 2022, **1203**, 339724.
12 N. Pourreza and K. Ghanemi, *J. Hazard. Mater.*, 2010, **178**(1–3), 566–571.
13 S. Gunduz, S. Akman and M. Kahraman, *J. Hazard. Mater.*, 2011, **186**(1), 212–217.
14 A. Sixto, A. Mollo and M. Knochen, *J. Food Compos. Anal.*, 2019, **82**, 103229.
15 M. Soylak, A. N. Çoban and H. E. H. Ahmed, *Food Chem.*, 2024, **442**, 138426.
16 Z. Wang, H. Wang, Z. Zhang, X. Yang and G. Liu, *Electrochim. Acta*, 2014, **120**, 140–146.
17 G. Chen, X. Hao, B. L. Li, H. Q. Luo and N. B. Li, *Sens. Actuators, B*, 2016, **237**, 570–574.
18 X. Wang, W. Lin, C. Chen, L. Kong, Z. Huang, D. Kirsanov, A. Legin, H. Wan and P. Wang, *Sens. Actuators, B*, 2022, **366**, 131922.
19 Y. M. Sung and S. P. Wu, *Sens. Actuators, B*, 2014, **201**, 86–91.
20 Y. Gan, T. Liang, Q. Hu, L. Zhong, X. Wang, H. Wan and P. Wang, *Talanta*, 2020, **208**, 120231.
21 G. Li, Q. Yang, X. Liu, L. Liu, J. Han and X. Li, *J. Photochem. Photobiol. Chem.*, 2024, **447**, 115228.
22 M. Maruthupandi, M. R. J. Stairish, S. Sahila and N. Vasimalai, *J. Mol. Struct.*, 2022, **1269**, 133798.
23 S. Ebrahim Mohammadzadeh, F. Faghiri and F. Ghorbani, *Microchem. J.*, 2022, **179**, 107475.
24 J. Charoensuk, J. Thonglao, B. Wichaiyo, K. Mukdasai, Y. Santaladchaiyakit, S. Srijaranai and S. Mukdasai, *Microchem. J.*, 2021, **160**, 105666.
25 P. A. Bazuła, P. M. Arnal, C. Galeano, B. Zibrowius, W. Schmidt and F. Schüth, *Microporous Mesoporous Mater.*, 2014, **200**, 317–325.
26 Y. Takeda, Y. Komori and H. Yoshitake, *Colloids Surf. A Physicochem. Eng. Asp.*, 2013, **422**, 68–74.

27 S. Metarwiwinit, S. Mukdasai, C. Poonsawat and S. Srijaranai, *New J. Chem.*, 2018, **42**(5), 3401–3408.
28 F. Accioni, D. García-Gómez, E. Girela and S. Rubio, *Talanta*, 2018, **182**, 574–582.
29 A. Galal, N. F. Atta and E. H. El-Ads, *Talanta*, 2012, **93**, 264–273.
30 M. J. Ahmed and M. T. I. Chowdhury, *Anal. Sci.*, 2004, **20**(6), 987–990.
31 N. Goudarzi, *J. Agric. Food Chem.*, 2009, **57**(3), 1099–1104.
32 B. N. Kumar, S. H. Kumar, G. G. Redhi and N. V. V. Jyothi, *Asian J. Chem.*, 2016, **28**(8), 1861–1866.
33 A. Thongsaw, W. C. Chaiyasith, R. Sananmuang, G. M. Ross and R. J. Ampiah-Bonney, *Food Chem.*, 2017, **219**, 453–458.
34 R. Sedghi, S. Kazemi and B. Heidari, *Sens. Actuators, B*, 2017, **245**, 860–867.
35 N. Thiagarajan and M. Subbaiyan, *Anal. Chim. Acta*, 1992, **269**(2), 269–272.
36 H. Fiedler, *Talanta*, 2004, **64**(1), 190–195.
37 B. E. Saltzman, *Anal. Chem.*, 1953, **25**(3), 493–496.
38 Md. R. Awual, Md. M. Hasan and H. Znad, *Chem. Eng. J.*, 2015, **259**, 611–619.
39 Md. R. Awual, T. Yaita, H. Shiwaku and S. Suzuki, *Chem. Eng. J.*, 2015, **276**, 1–10.
40 Md. R. Awual, T. Yaita, S. Suzuki and H. Shiwaku, *J. Hazard. Mater.*, 2015, **291**, 111–119.
41 K. M. Sachin, S. A. Karpe, M. Singh and A. Bhattarai, *R. Soc. Open Sci.*, 2019, **6**(3), 181979.
42 V. N. Mehta, H. Basu, R. K. Singhal and S. K. Kailasa, *Sens. Actuators, B*, 2015, **220**, 850–858.
43 P. Huang, B. Liu, W. Jin, F. Wu and Y. Wan, *J. Nanoparticle Res.*, 2016, **18**(11), 327.
44 Y. Dong, L. Ding, X. Jin and N. Zhu, *Microchim. Acta*, 2017, **184**(9), 3357–3362.